# Accepted Manuscript

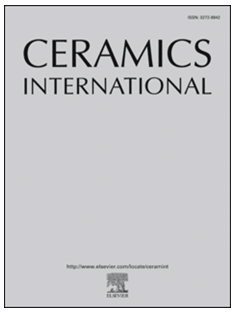


Iron oxidation state effect on the Mg-Al- Si-O glassy system

N.M. Ferreira, A. Sarabando, S. Atanasova-Vladimirova, R. Kukeva, R. Stoyanova, B.S. Ranguelov, F.M. Costa

PII: S0272-8842(19)31945-5

DOI: https://doi.org/10.1016/j.ceramint.2019.07.125

Reference: CERI 22240

To appear in: *Ceramics International*

Received Date: 11 June 2019

Revised Date: 10 July 2019

Accepted Date: 11 July 2019

Please cite this article as: N.M. Ferreira, A. Sarabando, S. Atanasova-Vladimirova, R. Kukeva, R. Stoyanova, B.S. Ranguelov, F.M. Costa, Iron oxidation state effect on the Mg-Al- Si-O glassy system, *Ceramics International* (2019), doi: https://doi.org/10.1016/j.ceramint.2019.07.125.

# Iron oxidation state effect on the Mg-Al- Si-O glassy system

N.M. Ferreira[1,2,*], A. Sarabando[2], S. Atanasova-Vladimirova[3], R. Kukeva[4], R. Stoyanova[4], B.S. Ranguelov[3] and F.M. Costa[1]

[1] i3N, Department of Physics, University of Aveiro, Aveiro, Portugal

[2] CICECO – Aveiro Institute of Materials, Department of Materials and Ceramic Engineering, University of Aveiro, Aveiro, Portugal

[3] Institute of Physical Chemistry, Bulgarian Academy of Sciences, Bulgaria

[4] Institute of General and Inorganic Chemistry, Bulgarian Academy of Sciences, Bulgaria

*: nmferreira@ua.pt

## Abstract

Mg-Al-Si-O glassy systems have a great importance in a wide range of industrial applications, specifically as an electrolyte for molten oxide electrolysis processes in steelmaking. Understanding how the iron oxidation state of the raw material ($Fe^{2+}/Fe^{3+}$) and its corresponding amount influence this glassy system's properties will be the aim of the current work. Iron oxides (as $Fe_2O_3$ or $Fe_3O_4$) were used to dope Mg-Al-Si-O system obtaining amorphous materials through an unconventional method: Laser Floating Zone (LFZ). Above 8 % mol of Fe formation of magnetic phases or iron clusters, were observed in the glass matrix. Samples with $Fe_2O_3$ showed a higher crystal concentration, when compared with $Fe_3O_4$. The electron paramagnetic resonance measurements show a strong dependence on the iron source ($Fe_3O_4$ or $Fe_2O_3$). In addition, the magnetization decreases linearly with iron content, independently of iron oxidation state, except for samples with a higher concentration of $Fe_2O_3$(15 % mol), due to sample crystallization. Moreover, with $Fe_3O_4$ as raw material there is an improvement (~ 250 times) of the electrical conductivity when compared with $Fe_2O_3$. The results show that the presence of $Fe^{2+}$ on the glass influences the electrical conductivity, which could have impact in the efficiency of molten oxide electrolysis process.

## Keywords

Mg-Al-Si-O glassy system; iron oxidation state; laser floating zone processing; iron doped glass

## Introduction

The system $MgO\text{-}Al_2O_3\text{-}SiO_2\text{-}FeO_y$ is mentioned in several works as an electrolyte basis for the molten oxide electrolysis process, in order to obtain molten Fe from its oxides. Furthermore, it is worth to mention that this composition is already presented as a slag in the iron extractive metallurgy processes [1-6]. There are already several studies that analyse the structural changes due to iron oxides, the corresponding impact on the magnetic, optical and catalytic properties and even some potential technological applications [1, 3-7]. However, there are still few works concerning the impact of iron on the electrical and magnetic properties in glass systems [8-11]. For the latter, redox conditions and temperature determine the iron oxides state and the crystalline phase content in the quaternary system $MgO\text{-}Al_2O_3\text{-}SiO_2\text{-}FeO_y$ [1, 3-11]. This redox process is due to the different oxidation states of iron in magnetite $Fe^{3+}[Fe^{3+}\ Fe^{2+}\ O_4]$ and hematite $Fe^{3+}[Fe^{3+}\ O_3]$ [12].

In order to understand the effect of iron oxidation state and the ratio between ($Fe^{2+}/Fe^{3+}$) on the properties of this glass system, amorphous samples were obtained with different iron content and oxidation states. This was possible by using the laser floating zone (LFZ) method, since this technique is suitable to work under non-equilibrium conditions. The pulling rate in the LFZ process is similar to the cooling rate in a conventional furnace, allowing a flexible control on the crystallization degree of the Fe-Mg-Al-Si-O materials and therefore affecting their properties [13-15].

Previous studies shows that it is possible to obtain fibres of Mg-Al-Si-O doped with iron under fast pulling rates [9]. Moreover, it has been shown that growth rate affects the iron oxidation in glass matrix [10]. These works describe the crystallization of the Fe-Mg-Al-Si-O glassy system and the effect of iron concentration on the phase composition. The results suggest that there are a complex crystallization /vitrification mechanisms occurring, controlled by the cooling conditions in LFZ and also by the network-forming capabilities of the $Fe^{2+}$ and $Fe^{3+}$ cations [9, 10]. It was found that the presence of a significant $Fe^{2+}/Fe^{3+}$ redox interactions on Mg-Al-Si-O glass and corresponding $Fe^{3+}$ fraction exert a noticeable effect on the electrical conductivity. The effects of $Fe^{2+}/Fe^{3+}$ on iron distribution and the local environment in the glass were also analysed. The conductivity and magnetic measurements showed the effect of the iron interaction with the glass matrix and its elements, being very important during the molten oxide electrolysis process.

The present work focuses in the influence of iron amount and its oxidation state on the crystallization of the glassy matrix and in the formation of the magnetic and non-magnetic phases. To study the effect of $Fe^{2+}$ and $Fe^{3+}$ cations on the crystallization process a magnetic and electrical characterization were performed.

## Experimental procedure

Commercial oxide powders of MgO (Merck, +99%), $Al_2O_3$ (Merck, 99.5%), $SiO_2$ (Sigma–Aldrich, 99.6%), $Fe_3O_4$ (Sigma–Aldrich, +98%) and $Fe_2O_3$ (Aldrich, +99%) were mixed to obtain samples with nominal composition ($Mg_{0.203}$ $Al_{0.374}$ $Si_{0.423}$ $O_{1.61}$), containing 0, 2, 4, 8 and 15 % mol of iron cations. A binder (PVA – Polyvinyl alcohol) was added to the power mixture in order to extrude the powers as cylindrical rods. These extruded rods were used as a feed and seed in the LFZ growth system as described in [11]. The LFZ system is equipped with a continuous $CO_2$ Spectron SLC laser (λ = 10.6 μm; 200 W) and a growth rate of 100 mm/h was used. In order to improve the homogeneity of the fibres, the seed and feed rod precursors rotated in opposite directions. Figure 1 presents the as-grown samples, and for those with iron concentrations below 8 %mol the brightness aspect is quite visible. Taking into account the iron oxidation states, no effects are visible.

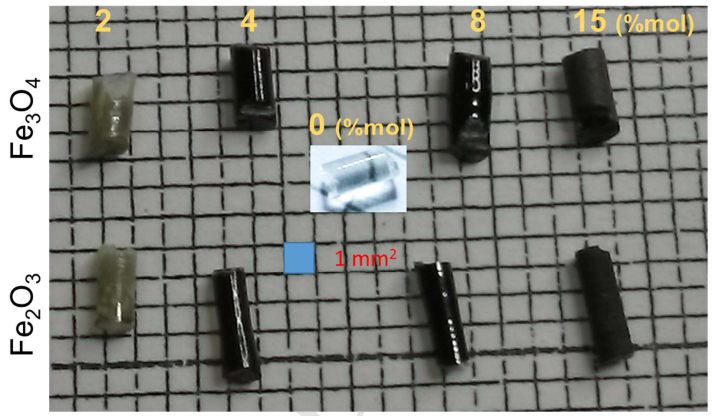


Fig 1 – Visual appearance of the samples and influence of iron content and oxidation state.

X-ray diffraction (XRD) was performed in powder samples using a Panalytical X'pert PRO3 diffractometer (CuKa1 radiation). The obtained diffraction patterns were analysed using a JCPDS database to identify the phases present in the samples.

Sample morphology and elemental composition were analysed by scanning electron microscopy and energy dispersive analyser in a JEOL JSM 6390, equipped with an INCA Oxford EDS detector.

The iron oxidation state was determined by a Bruker EMX$^{plus}$ EPR spectrometer, operating in the X-band (i.e. at 9.4 GHz) for temperature range from 100-500 K. The measurements were done using quartz tubes.

DC magnetic measurements were performed on bulk fibre samples (50– 100 mg) using a vibrating sample magnetometer (VSM) from Cryogenic Cryofree. The DC magnetization was recorded on Zero field cooled (ZFC) and field-cooled (FC) under 0.1 T, from 5 to 300 K. Typical hysteresis curves were measured at 5 and 300 K, for all samples in magnetic field up to 5 T in a parallel position to the applied magnetic field.

Electrical response of the samples at room temperature was monitored by DC measurements in a suitable homemade 4-point probe resistivity setup, comprising an ISO-Tech programmable power supply IPS603 and a HP Multimeter 34401A. On the top of the fibres, Ag paste was applied to provide suitable electrical contact.

## Results and Discussion

The XDR analysis of pure and iron-doped as-grown samples placed in evidence an amorphous structure (Fig 2), independently of the oxidation state of the raw material. The presence of crystalline phases was detected only for the higher iron content (15 % mol), as observed by the peaks intensities and widths on the XRD patterns (Fig 2). However, it is important to highlight that the nature of crystalline phases depends strongly on the oxidation state of iron in the raw material.

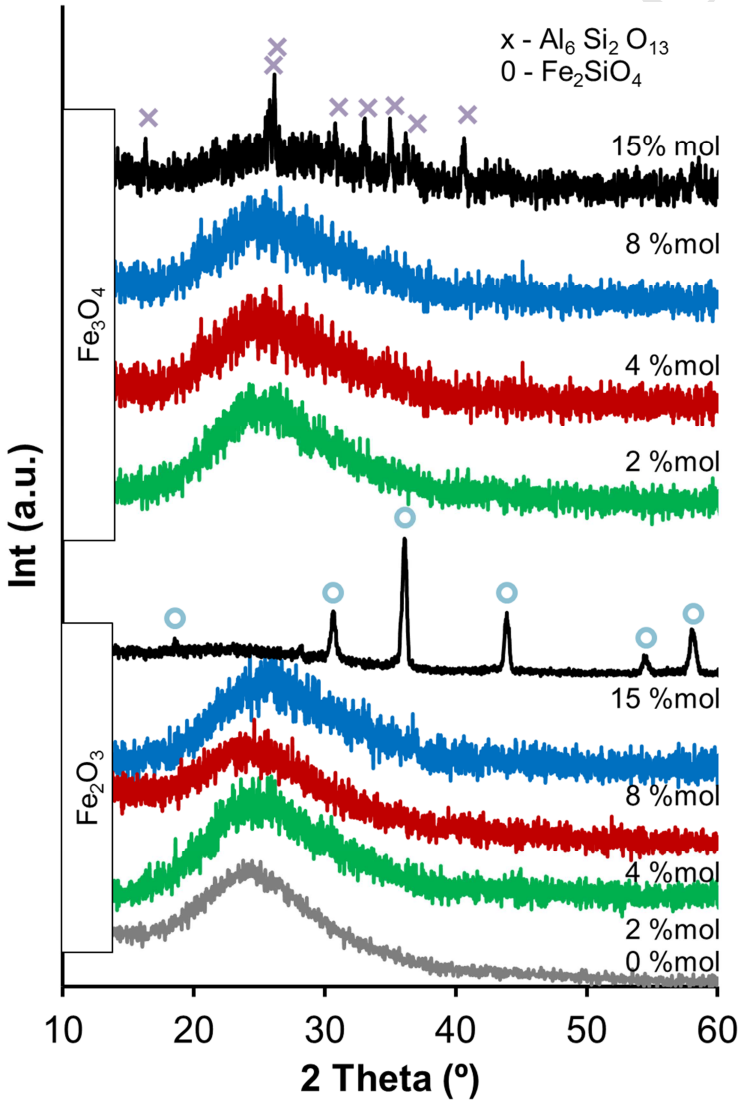


Figure 2 – XRD patterns of powdered samples doped with $Fe_3O_4$ and $Fe_2O_3$, respectively.

In fact, the sample obtained from hematite ($Fe_2O_3$) exhibits a superior crystallization degree. This result clearly shows the iron oxidation state ($Fe^{2+}$ and $Fe^{3+}$) influence the crystallization process for samples with the same iron content, since different degrees of crystallization and phases occur. For fibres with $Fe_3O_4$ (and 15 % mol of Fe) a mullite ($Al_6Si_2O_{13}$) phase was detected (ref card: 00-015-0776), with an orthorhombic crystalline structure (space group of Pbam) and the following lattice parameters: a = 7.5456 Å, b = 7.6898 Å and c = 2.8842 Å. The presence of this phase was previous detected in this glass system when grown at a lower pulling rates (10-50 mm/h) and lower iron concentrations (0 and 2 % mol) [9]. Iron silicate ($Fe_2SiO_4$) phase (ref card: 01-080-1625) with a cubic structure (space group of Fd-3m) and a lattice parameter of 8.2413 Å was detected for the higher amount of $Fe_2O_3$ (15 % mol of Fe).

The distinct crystallization degree observed in fibres obtained with different iron oxidation states (Fig 2) could be due to the role of $Fe^{2+}$ and $Fe^{3+}$ cations on the crystallization process, namely how they interact with the glassy matrix. Indeed, $Fe^{2+}$ generally acts as a network modifier, while $Fe^{3+}$ could act both as a network former and as a network modifier [10]. Previous work already substantiated that the iron interaction with the glass matrix is more noticeable at lower pulling rates, due to variations of the iron oxidation state and the formation of clusters in the glass matrix [10].

SEM analysis confirmed the absence of crystallinity in the samples with an iron concentration below 15 % mol (not shown). Also, no crystals were observed in the fracture and cross section of the samples, and they seem homogeneous. In contrast, the samples with a higher iron concentration (15 % mol) presented formation of crystals, as shown in figure 3, confirming the XRD results. The chemical characterization (EDS) confirms the phases composition detected by XRD. The samples with $Fe_2O_3$ presents a higher concentration of crystals (Fig. 3) when compared to the one with $Fe_3O_4$, which explains the peaks' intensity of the corresponding XRD patterns.

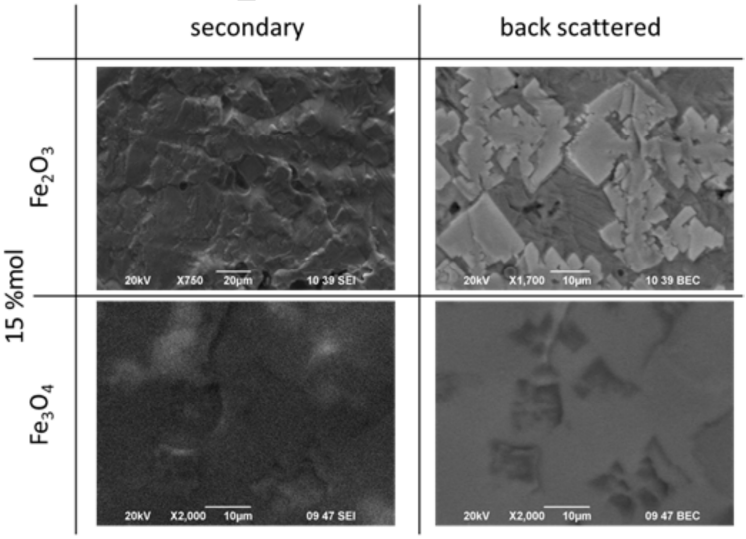


Figure 3 -Micrographs of samples with 15 % mol of iron, grown at 100 mm/h using $Fe_2O_3$ and $Fe_3O_4$ as source of iron.

In order to understand the effect of $Fe^{2+}$ and $Fe^{3+}$ cations on the crystallization process a detailed magnetic characterization was performed using electron paramagnetic resonance and magnetization measurements. Figure 4 displays the EPR spectra of low and high iron doped glasses. The EPR spectra of low doped glasses consist of two signals: a narrow signal for $g \sim 4.3$ and a broad signal for $g \sim 2$. The signal with $g \sim 4.3$ is typical for isolated $Fe^{3+}$ ions that are located in the crystal with a rhombic symmetry [16, 17, 18]. While the broad signal with $g \approx 2$ could be attributed to non-isolated $Fe^{3+}$ ions that are coupled by magnetic interactions [16-18]. The similar EPR profiles for $Fe_3O_4$- and $Fe_2O_3$-doped glasses reveal that iron ions have one and the same coordination regardless of the used raw material. For highly doped glasses the EPR spectra profiles undergo strong changes and they become dependent on the kind of iron source used (i.e., $Fe_3O_4$ or $Fe_2O_3$) [17]. Two features can be outlined: first, the signal with $g \sim 4.3$ due to isolated $Fe^{3+}$ ions disappears completely when change from low to high $Fe_2O_3$ and $Fe_3O_4$-doped glasses. Second, the broad signal with $g \approx 2$ grows in intensity with an increase of the iron content and its shape is different for $Fe_2O_3$ or $Fe_3O_4$, when used as an iron source [17].

For the $Fe_2O_3$-doped system, the EPR spectrum displays an asymmetric signal with an apparent *g*-value of 2.05 and line width of 64 mT. On cooling down from 295 K to 120 K, the signal becomes broader and shifts to lower magnetic fields. In comparison with $Fe_2O_3$-doped glasses, a broader signal is observed in the EPR spectrum of $Fe_3O_4$-doped glasses, with an apparent *g*-value and line width of 2.2 and 125 mT, respectively. This signal is shifted to lower magnetic fields, concomitant with a line broadening when the temperature decreases from 295 to 120 K. It is worth mention that the EPR spectra of iron-doped glass systems are quite different from that for the raw oxides $Fe_2O_3$ and $Fe_3O_4$. This is a direct evidence of the full integration of iron oxides into the glass matrices [16-18]. Therefore, the self-consistent change in the line position and line width of the broad signal can be related with the formation of superparamagnetic iron-containing clusters [16, 17, 18].

The disappearance of the signal of isolated $Fe^{3+}$ ions at $g \sim 4.3$ with increase of iron content, as well as the increase in the broad signal with $g \approx 2$, are in agreement with EPR data reported in the literature for glass matrices containing iron in a concentration range of 0 – 8 % mol [10]. It is assumed that the signal at $g \sim 4.3$ is a fingerprint of isolated $Fe^{3+}$ ions in the glass network and they may be combined in various structural arrangements [18-21]. At the same time, the line in higher magnetic fields ($g \sim 2.0$) may be attributed to the formation of clusters containing $Fe^{3+}$ [10, 18, 19, 22], and the increase in the signal intensity at $g \sim 2.0$ can be assumed as an indication of progressive clustering [10, 23]. These clusters can be quite complex due to formation of $Fe^{3+}$-$Fe^{2+}$ or $Fe^{3+}$-$Fe^{3+}$pairs, with possible super-exchange and dipole-dipole interactions [10, 23].

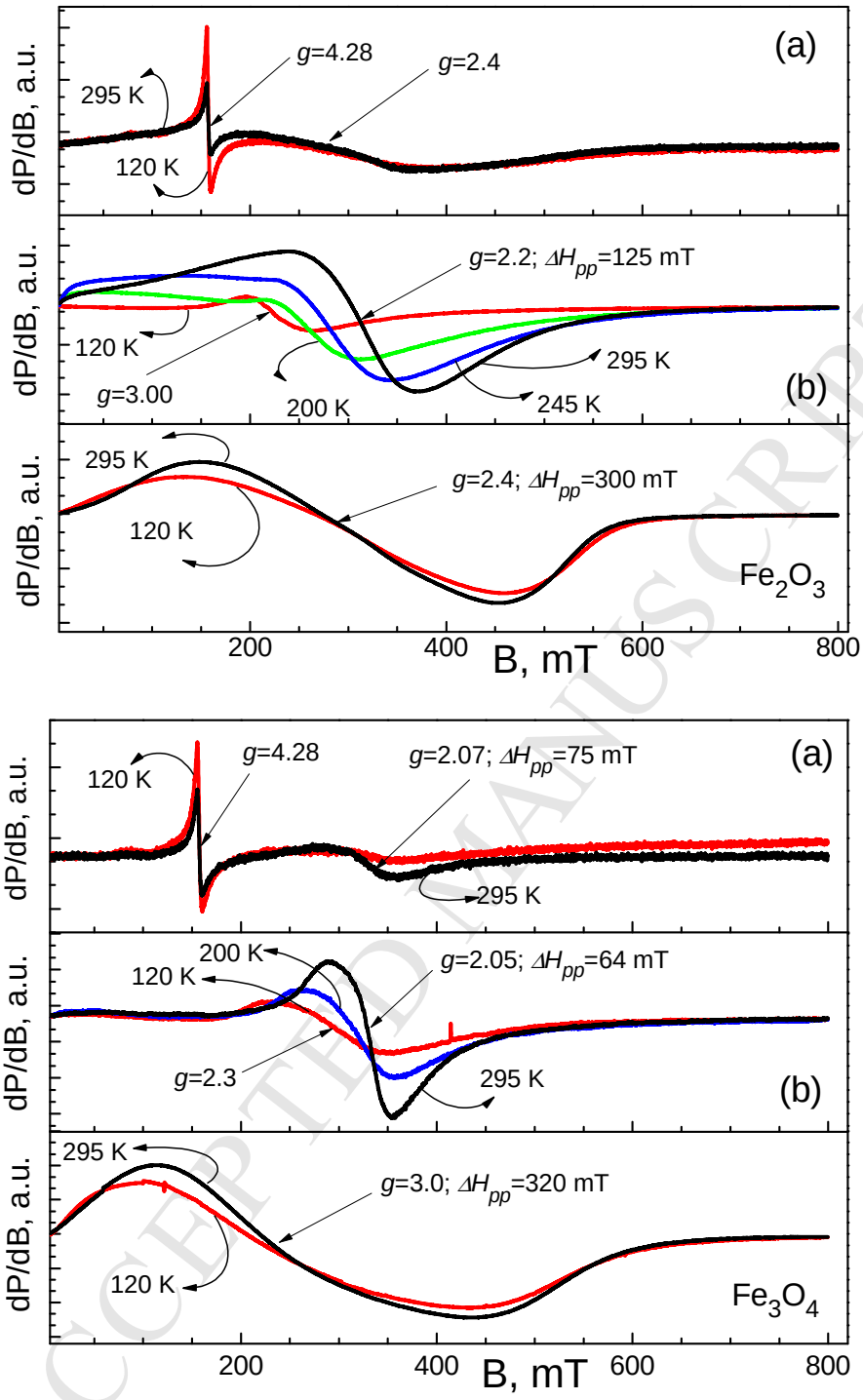


Figure 4 - EPR spectra of 2%mol (a) and 15 % mol (b) of $Fe_2O_3$ (up) and 2% mol (a) and 15% mol (b) of $Fe_3O_4$, (down). In the interest of comparison, the EPR spectra of raw $Fe_2O_3$ and $Fe_3O_4$ are also shown.

The EPR results are corroborated by the magnetization measurements (Figs 5), where at low temperature it is observed a hysteresis loop for all samples (Fig 5a), except for the one with 2 % mol of $Fe_2O_3$, that presents a paramagnetic behaviour, therefore confirming a lower iron concentration [24]. Magnetic measurements at room temperature show the samples' paramagnetic behaviour (Fig 5b), except for the sample

with 15 % mol of $Fe_2O_3$, that presents a superparamagnetic behaviour with higher magnetization value. This outcome confirms the EPR results and it is in accordance with other reported findings for this crystalline structure ($Fe_2SiO_4$ - magnetic phase) [25]. The remaining samples show magnetization values and behaviour typical of glass systems containing iron [9, 10, 18]. A linear decrease of the magnetization value with the iron content (fig 5a-b) is observed, independently of its oxidation state.

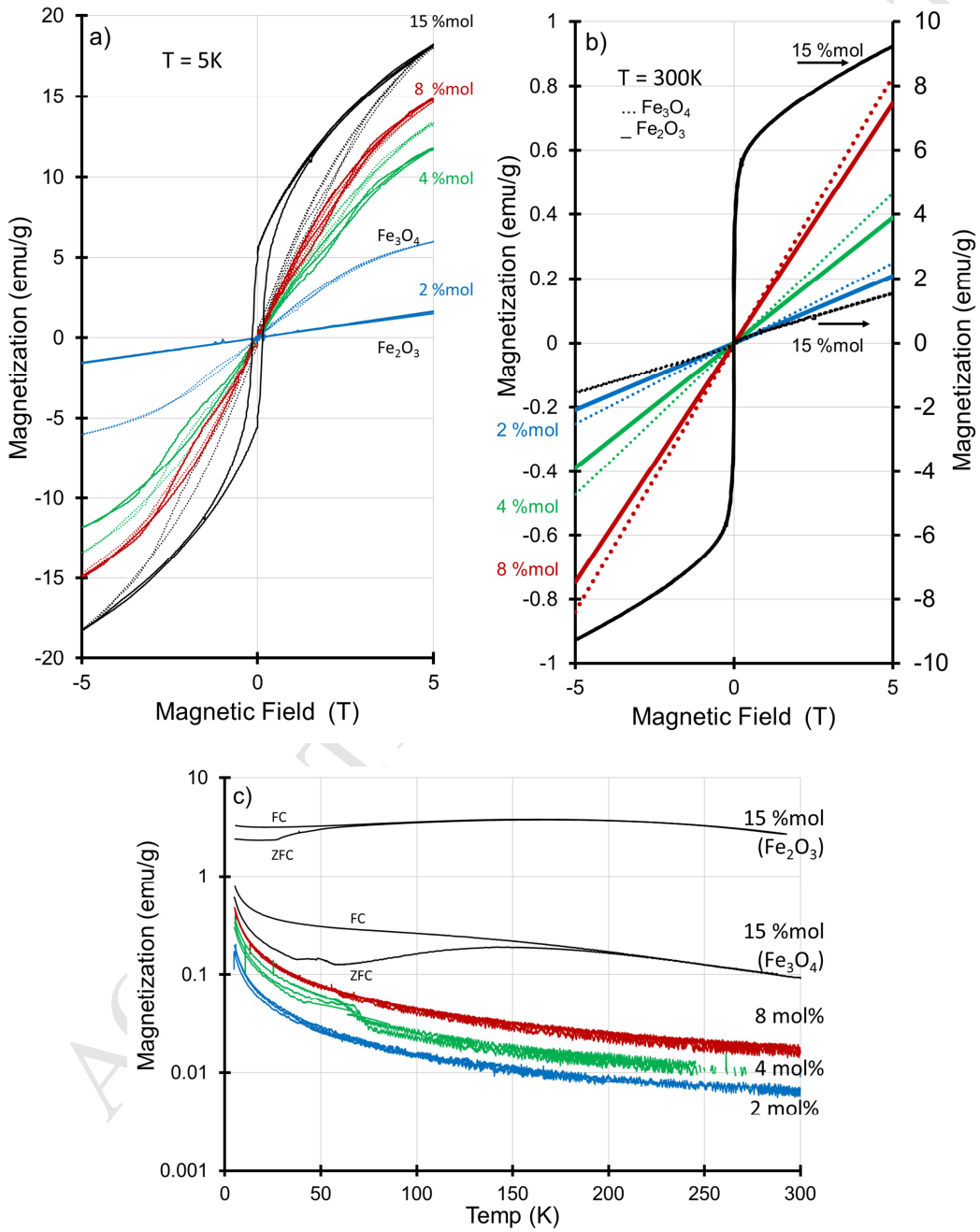


Figure 5 –Magnetization measurements for samples with x= 0 - 15 % mol Fe and different iron raw materials: $Fe_2O_3$ (line___) and $Fe_3O_4$ (dots.....).

The magnetization decreases from 5 to 300 K (Fig 5c) for samples with low iron concentration (<15 % mol). The decrease of magnetization is more drastic from 5 to 20 K, while at higher temperatures the decrease is slower for all samples. Such behaviour is due to the iron concentration and how the iron interacts/distributes itself in the glassy matrix [18]. The temperature behaviour for the 15 % mol $Fe_2O_3$ sample confirms the presence of the $Fe_2SiO_4$ crystals [25] and it is possible to observe a constant value all along the temperature range (Fig 5c).

The iron amount and oxidation state influences the magnetization behaviour, and it is more visible in the hysteresis cycle at 5 K for a lower iron concentration. At high temperatures and for higher iron concentrations, the influence of $Fe^{2+}/Fe^{3+}$ is more noticeable, due to the presence of magnetic crystals such as $Fe_2SiO_3$ that influence the magnetization values and behaviour as observed in Figs. 5 [12, 18].

Moreover, samples with 15 % mol of $Fe_2O_3$, show transitions between the measurements on ZFC (Zero Field Cold) and FC (Field Cold) method at T ~ 60 K, while for $Fe_3O_4$ samples such transitions are observed at T ~ 160 K (Fig 5c). This could be due to the iron oxidation state and also to how the iron interacts with the matrix (formation of clusters) [10, 18].

Additionally, an electric characterization was performed in order to deeply understand the features of this system. The results of electric measurements confirm the presence of a glass matrix with the incorporation of an element that behaves like an electric conductor (Fig. 6). This result are in accordance with the values reported for the same glass system [9, 10]. Moreover, it is observed that a higher Fe concentration improves the electrical conductivity in all samples. In addition, when $Fe_3O_4$ is used as raw material the electrical conductivity improves 250 times upon comparison with the use of $Fe_2O_3$. The reason for this higher electrical conductivity could be due to how iron ions interact with the glass matrix and how they are dispersed. While for lower concentrations it is observed a low electrical conductivity due to how the ions being dispersed in the glass matrix. For a higher iron content the presence of clusters could explain, the increase of electrical conductivity and the mechanism of electrical conduction in this material.

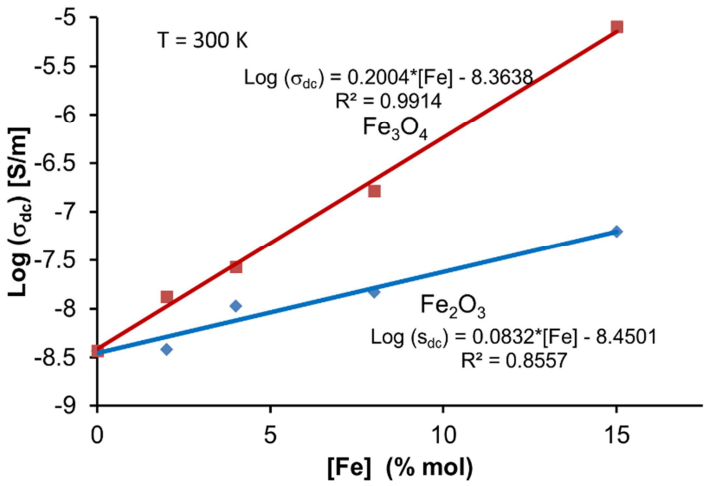


Figure 6 – Electrical conductivity (DC) measurements of samples at room temperature

The significant changes in the oxidation state and preferred coordination of iron cations observed above 8 % mol iron concentration are correlated with the significant increase in conductivity. This result could be due to a contribution from $Fe^{2+}/Fe^{3+}$ redox interactions and clustering, a possibility supported by EPR results and also by the increase of magnetization. This outcome might result in an appearance of redox-driven polaron conduction mechanisms in this MAS glass system, by hopping between $Fe^{2+}$ and $Fe^{3+}$ cations [11].

Inferring from the presented results, it is observed the influence of $Fe^{2+}$ on electrical and magnetic properties, whereas the electrical conductivity and magnetization both suffer an increase with the iron concentration. Moreover, the influence of the iron oxidation state on the raw material is more evident for higher iron concentrations.

## Conclusions

The LFZ method was successfully used in the present work to grow amorphous materials in order to study the effect of iron doping in the Mg-Al- Si-O glass system. For growth rates of 100 mm/h, amorphous materials were obtained below 8 % mol of iron content, regardless of the oxidation state ($Fe^{2+}/Fe^{3+}$). In opposition, 15 % mol of iron concentration induces crystallization of the samples, with magnetic and non-magnetic phases, due to how $Fe^{2+}$ and $Fe^{3+}$ interact with the glass matrix.

The magnetic measurements (VSM and EPR) confirm the results of the structural characterization and demonstrate the influence of iron oxidation states on magnetic behaviour, as well as the formation of clusters with a higher iron concentration. The electrical measurements reveal the influence of the ($Fe^{2+}/Fe^{3+}$) ratio and concentration on conductivity. Moreover, using $Fe_3O_4$ as raw material increases almost 250 times the electrical conductivity.

From the present results, for lower iron concentrations (< 8 % mol) the oxidation state did not reveal a significant influence on electrical and magnetic properties. However, for higher concentrations (15 % mol), the effect is more pronounced, because the iron oxidation state promotes the formation of magnetic phases and iron clustering in the glass matrix.

## Acknowledgements

The work is being carried out in the scope of project UID/CTM/50025/2013, funded by the FCT-MCTES and co-funded by the FEDER under the PT2020 partnership agreement. Nuno Ferreira acknowledges the fellowship grant SFRH/BPD/111460/2015. This work is funded by national funds (OE), through FCT – Fundação para a Ciência e a Tecnologia , I.P., in the scope of the framework contract foreseen in the numbers 4, 5 and 6 of the article 23, of the Decree-Law 57/2016, of August 29, changed by Law 57/2017, of July 19.

Bogdan Ranguelov acknowledges the support of Project INFRAMAT - D01-155/28.08.2018, funded by the Bulgarian Ministry of Education and Science

## References

[1] A. Allanore, Electrochemical engineering of anodic oxygen evolution in molten oxides, Electrochim. Acta 110 (2013) 587-592. http://dx.doi.org/10.1016/j.electacta.2013.04.095.

[2] D.R. Sadoway, New opportunities for waste treatment by electrochemical processing in molten salts, in K.C. Liddell, R. G. Bautista and R.J. Orth, The Minerals, Metals & Materials Society, (1994) 73-76, ISBN Number: 0-87339-244-2.

[3] S.X. Wang, L.M. Wang, R.C. Ewing, R.H. Doremus, 1998. Ion beam-induced amorphization in MgO-Al2O3-SiO2. I. Experimental and theoretical basis, J. Non-Cryst. Solids 238 (1998) 198-213, doi: 10.1016/S0022-3093(98)00694-2.

[4] I.H. Jung, S.A. Decterov, A.D. Pelton, A.D., Critical Thermodynamic Evaluation and Optimization of the FeO – Fe2O3 – MgO – SiO2 System, Metall. Mater. Trans. B 35B (2004) 877-889, doi: 10.1007/s11663-004-0082-9.

[5] D. Wang, A.J. Gmitter, D.R. Sadoway, Production of oxygen gas and liquid metal by electrochemical decomposition of molten iron oxide, J. Electrochem. Soc. 158 (2011) E51-E54.

[6] Z.H. Jiang, S.J. Li, Y., Thermodynamic calculation of inclusion formation in Mg-Al-Si-O system of 430 stainless steel melts, Journal of Iron and Steel Research International 18 (2011) 14-17, doi: 10.1016/S1006-706X(11)60017-4

[7] R. Kaindl, D.M. Többens, U. HaefeKer, Quantum-mechanical calculations of the Raman spectra of Mg- and Fe-cordierite, Am. Mineral. 96 (2011) 1568–1574, doi: 10.2138/am.2011.3845

[8] M.D. Ingram, Superionic glasses: theories and applications. Current Opinion in Solid State & Materials Science 2 (1997) 399-404, doi: 10.1016/S1359-0286(97)80079-4

[9] N.M. Ferreira, A.V. Kovalevsky, M.A. Valente, J.C. Waerenborgh, J.R. Frade, F.M. Costa, Structural and redox effects in iron-doped magnesium aluminosilicates. Journal of Crystal Growth 457 (2017) 19–23, DOI: 10.1016/j.jcrysgro.2016.01.039.

[10] N.M. Ferreira, A.V. Kovalevsky, M.A. Valente, N.A. Sobolev, J.C. Waerenborgh, F.M. Costa, J.R. Frade, Iron incorporation into magnesium aluminosilicate glass network under fast laser floating zone processing. Ceramics International 42 (2016) 2693-2698, DOI: 10.1016/j.ceramint.2015.10.150.

[11] N.M. Ferreira, A.V. Kovalevsky, J.C. Waerenborgh, M. Quevedo-Reyes, A.A. Timopheev, F.M. Costa, J.R. Frade, Crystallization of iron-containing Si–Al–Mg–O glasses under laser floating zone conditions. Journal of Alloys and Compounds 611 (2014) 57–64, DOI: 10.1016/j.jallcom.2014.05.118.

[12] R. Muller, H. Fuess, P. Brown. Magnetic Properties of Synthetic Fayalite (α-Fe2SiO4. Journal de Physique Colloques, 43 (1982) C7-249-C7-252, doi: 10.1051/jphyscol:1982735.jpa-00222342.

[13] Jürn W.P. Schmelzer, Alexander S. Abyzov, Vladimir M. Fokin, Christoph Schick, Edgar D. Zanotto, Crystallization of glass-forming liquids: Maxima of nucleation, growth, and overall crystallization rates, J. Non-Cryst. Sol. 429 (2015) 24–32, doi:10.1016/j.jnoncrysol.2015.08.023.

[14] M.F. Carrasco, R.F. Silva, J.M. Vieira and F.M. Costa, Pulling rate and current intensity competition in electrically assisted laser floating zone, Supercond. Sci. Technol. 22 (2009) 065016. http://dx.doi.org/10.1088/0953-2048/22/6/065016

[15] F.M. Costa, N.M. Ferreira, S. Rasekh, A.J.S. Fernandes, M.A. Torres, M.A. Madre, J.C. Diez, A. Sotelo, Very Large Superconducting Currents Induced by Growth Tailoring. Crystal Growth & Design 15 (2015) 2094–2101, doi: 10.1021/cg5015972.

[16] D. L. Griscom, Electron spin resonance in glasses, J. Non-Cryst. Solids 40 (1980) 211-272, doi: 10.1016/0022-3093(80)90105-2.

[17] N. Guskos, G. J. Papadopoulos, V. Likodimos, S. Patapis, D. Yarmis, A. Przepiera, K. Przepiera, J. Majszczyk, J. Typek, M. Wabia, K. Aidinis, Z. Drazek, Photoacoustic,

EPR and electrical conductivity investigations of three synthetic mineral pigments: hematite, goethite and magnetite, Mater. Res. Bull. 37 (2002) 1051, https://doi.org/10.1016/S0025-5408(02)00742-0

[18] A.N. Vasiliev, L.V. Shvanskaya, O.S. Volkova, A.V. Koshelev, E.A. Zvereva, G.V. Raganyan, I.A. Presniakov, A.V. Sobolev, A.M. Abakumov, Y.M. Lvov, Magnetism of natural composite of halloysite clay nanotubes Al2Si2O5(OH)4 and amorphous hematite $Fe_2O_3$, Materials Characterization 129 (2017) 179-185, doi: 10.1016/j.matchar.2017.04.028.

[19] E.S. Dunaeva, I.A. Uspenskaya, K.V. Pokholok, V.V. Minin, N.N. Efimov, E.A. Ugolkova, E. Brunet, Coordination and RedOx ratio of iron in sodium-silicate glasses, J. Non-Cryst. Sol. 358 (2012) 3089–3095, doi: 10.1016/j.jnoncrysol.2012.08.004.

[20] M.D. Dyar, M.T. Naney, S.E. Swanson, Effects of quenching methods on Fe3+/Fe2+ ratios: A Mössbauer and wet-chemical study, Am. Miner. 72 (1987) 792-800.

[21] K.D. Jayasuriya, H.St.C. O'Neill, A.J. Berry, S.J. Campbell, A Mössbauer study of the oxidation state of Fe in silicate melts, Am. Miner. 89 (2004) 1597-1609, doi: 10.2138/am-2004-11-1203.

[22] S. Tadeu dos Reis, W. M. Pontuschka, J.B. Yang, D.L.A. Faria, Properties and Structural Features of Iron Doped BABAL Glasses, Materials Research 6 (2003) 389-394, doi: 10.1590/S1516-14392003000300013.

[23] - M. Elisa, R. Iordanescu, B. A. Sava, G. Aldica, V. Kuncser, C. Valsangiacom,G. Schinteie, F. Nastase, C. Nastase, V. Bercu, A. Volceanov, S. Peretz, Optical and structural investigations on iron-containing phosphate glasses, J Mater Sci 46 (2011) 1563–1570. DOI 10.1007/s10853-010-4963-9.

[24] - J. Kaewkhao, W. Siriprom, S. Insiripong, T. Ratana, C. Kedkaew, P. Limsuwan, Structural and Magnetic Properties of Glass Doped with Iron Oxide, Journal of Physics: Conference Series 266 (2011) 012012, doi:10.1088/1742-6596/266/1/012012.

[25] - T. Yamanaka, M. Okita, Magnetic properties of the Fe2SiO4-Fe3O4 spinel solid solutions, Phys Chem Minerals 28 (2001) 102-109, doi: 10.1007/s002690000.